Original Research

Investigation of Longitudinal Vascular Changes in Control and Chemotherapy-Treated Tumors to Serve as Therapeutic Efficacy Predictors

Min-Ying Su, PhD, Zhiheng Wang, PhD, and Orhan Nalcioglu, PhD

The impact of chemotherapy on longitudinal vascular changes taking place during the growth of an animal tumor, R3230 AC adenocarcinoma, was investigated. Two contrast agents of different molecular weights, gadolinium-diethylene-triamine-pentaacetic acid (Gd-DTPA; <1 kD) and gadomer-17 (35 kD), were used in the dynamic imaging studies. Enhancement kinetics were analyzed by a pharmacokinetic model to derive parameters related to vascular volume and permeability on a pixel-by-pixel basis. Responders and non-responders were separated according to tumor size 10 days after the therapy. Changes in the vascular volume measured by gadomer-17 at 4 days after therapy revealed a clear distinction between the controls and the responders/non-responders. Mean vascular volume decreased by 42% in responders but was not significantly changed in the controls. The one non-responder had increased vascular volume after chemotherapy. Enhancement kinetics of gadomer-17 detected the changes earlier and with greater sensitivity than Gd-DTPA. In the control group, vascular permeability determined by gadomer-17 correlated with the longitudinal growth rates of tumors, suggesting that vascular permeability assessed by gadomer-17 could potentially serve as an indicator of aggressive tumor growth. J. Magn. Reson. Imaging 1999; 9:128–137. © **1999 Wiley-Liss, Inc.**

Index terms: vascular volume; vascular permeability; chemotherapy; pharmacokinetic analysis; therapy efficacy; MR contrast agents

DYNAMIC gadolinium-diethylene-triamine-pentaacetic acid (Gd-DTPA)-enhanced tumor imaging can provide information about the extent of tumor necrosis and viability, which may serve as early predictors for the efficacy of chemotherapy in patients with bone or soft-tissue sarcomas (1–3). However, other parameters such as vascular volume and permeability may provide even earlier and more specific information about the response of tumor to therapy, thereby enabling the clinician to modify the treatment regimen after the initial cycle of chemotherapy has been administered. Measurement of vascularity and permeability of tumors by magnetic resonance imaging (MRI) has achieved some success in differentiating between benign and malignant tumors (4) and in determining the aggressiveness of tumor growth (5,6), which maybe influenced by vascular permeability factor/vascular endothelial growth factor (VPF/VEGF) (7,8). Vascular permeability has also been shown to be influenced by radiation therapy, as measured by dynamic contrast-enhanced MRI with albumin-Gd-DTPA (9,10). We therefore hypothesized that measurement of vascularity and permeability parameters shortly after therapy may provide an index of early vascular changes that precede the necrosis or volumetric changes commonly used to predict therapeutic outcome (11).

Information on vascular volume and permeability can be derived from pharmacokinetic modeling analysis of the intratumor kinetics of MR contrast agents. After intravenous injection of a contrast agent, it initially occupies the vascular space, and then diffuses into the interstitial space. We have previously developed pharmacokinetic analysis techniques that model the distribution of the contrast agents between these two compartments (12). After vascular and interstitial contributions are separated, the derived parameters can be used to characterize the vascular volume and permeability quantitatively. Since this technique is non-invasive, the tumor can be monitored longitudinally over a period of time to study the structural and vascular changes occurring during its growth and the alterations induced by various kinds of therapy.

In this work we studied the impact of chemotherapy on the longitudinal pharmacokinetic changes during the growth of an animal tumor, R3230 AC adenocarcinoma. To study the accuracy of vascular parameters derived from pharmacokinetic modeling, we employed two different sizes of contrast agents in the study. An extracellular agent, Gd-DTPA, was compared with a macromolecular blood-pool agent, gadomer-17 (intermediate size with an apparent molecular weight of 35 kD). These two agents were chosen because gadomer-17 mainly stays in the vascular space of the body but may also diffuse into the interstitial space depending on the degree of vascular permeability. Thus, gadomer-17 is

Health Sciences Research Imaging Center, College of Medicine, University of California, Irvine, California 92697–5020.

Contract grant sponsor: State of California Breast Cancer Research Program; contract grant number: 1RB-0160.

Presented at the 5th ISMRM meeting, 1997.

Address reprint requests to: O.N., Health Sciences Research Imaging Center, College of Medicine, University of California, Irvine, CA, 92697–5020. E-mail: NALCI@UCI.EDU

Received February 18, 1998; Accepted June 11, 1998.

expected to provide more reliable information about the vascular volume and permeability. On the other hand, we also used a smaller agent, Gd-DTPA, to investigate the extent of information that can be obtained from the kinetics of small agents. The longitudinal vascular changes were compared among the controls, responders, and non-responders. Response to chemotherapy was classified according to the volumetric growth rates of the tumors. We then determined which parameter most clearly differentiated between responders, non-responders, and controls. Such a parameter may serve as a predictor of therapeutic efficacy. We also evaluated which parameter correlated best with tumor growth to develop an early indicator of tumor aggressiveness. The parameters derived from the kinetics of Gd-DTPA were compared with the results obtained from the kinetics of gadomer-17. To date, Food and Drug Administration-approved MR contrast agents for human use all have low molecular weights. We therefore also focused our attention on the low molecular weight agent so that our interpretation of its kinetics would be clinically relevant.

MATERIALS AND METHODS

Tumor Model and Experimental Procedure

The experiments were performed on female Fischer 344 rats (weighing160 $\pm$ 10 g) bearing the R3230 AC adenocarcinoma. R3230 AC tumor cells were obtained from Dr. R. Weissleder (Massachusetts General Hospital) in 1996 and maintained by serial animal passages in our laboratory. The tumor was implanted by injecting 0.5 mL of minced tumor cell suspension (approximately 1×10^7 cells) subcutaneously into the left thigh of the rat. Fifteen animals were used in the study, nine in the treatment group and six in the control group. Baseline experiments started at 16 days post implantation. Averaged tumor volume at that time was 2.7 $\pm$ 1.2 mL as determined from baseline MRI.

The imaging protocol included T_2-weighted sequences across the entire tumor to measure both viable and non-viable tumor volumes, and a dynamic T_1-weighted sequence with sequential injections of Gd-DTPA (0.1 mmol/kg, Magnevist®, Berlex, Montville, NJ), followed by gadomer-17 (0.05 mmol/kg, provided by Schering, Berlin, Germany) to measure the enhancement kinetics in the tumor. Gadomer-17 is a synthetic dendrimeric gadolinium chelate, with a nominal molecular weight of 17 kD and an apparent molecular weight of about 35 kD, (i.e., it has a Stokes' radius similar to a protein of 35 kD). The molar relaxivity of gadomer-17 was about 3.5 to 4.5 times that of Gd-DTPA and was generally independent of field strength (Dr. Weinmann of Schering, personal communication). Plasma values were almost identical, which implied minimal protein binding. In rats the LD_{50} was greater than 20 mmol/kg body weight, and completed renal elimination occurred within 24 hours.

Chemotherapy was administered to animals in the treatment group 3 days after the baseline study. Mitomycin-C (5 mg/kg; Bristol-Myers Squibb, Princeton, NJ) was first injected i.p., and then 1 hour later a vessel-occluding agent, flavone acetic acid (FAA; 200 mg/kg, provided by the Drug Synthesis and Chemical Branch, National Cancer Institute) was injected. Four days after the chemotherapy, i.e., 1 week after the baseline study, the imaging experiments were repeated (noted as the first follow-up, or week-1 study). After the second week the third imaging experiments were conducted (noted as the second follow-up, or week-2 study).

Imaging experiments were performed on a GE Signa 1.5 T Scanner with a GE linear head coil. Each animal was anesthetized by injecting 50 mg/kg ketamine mixed with 5 mg/kg Rompun intramuscularly into the front limb. A 25 gauge butterfly cannula was then inserted into the tail vein for injection of contrast agent. Animals were fastened to paper boards in the lateral decubitus position and placed into the center of the coil. A fast spin-echo pulse sequence (TR 3 s, TE 112 msec, 8 echo train, interleaved 3 mm slice) was applied to acquire T_2-weighted images across the whole tumor. Three axial slices (5 mm thick), one from liver and two from tumor, were then selected for the dynamic study. Enhancement kinetics in the liver were measured to study any possible systemic changes in the host animal that could affect the pharmacokinetic changes in the tumor. A T_1-weighted spin-echo pulse sequence with TR/TE 120/18 msec was applied to acquire dynamic images of the three slices simultaneously, as described previously (13). After four baseline images had been acquired for each slice, Gd-DTPA (0.1 mmol/kg) was injected into the rat. Enhancement kinetics were monitored for 17 minutes. After waiting 1 hour to allow for the clearance of Gd-DTPA (more than 90%), gadomer-17 (0.05 mmol/kg) was injected and the kinetics were monitored for 17 minutes. After the imaging studies were completed, animals were sent back to their housing facility for the scheduled treatment and the follow-up studies.

Data Analysis

All data analyses were performed on a Sun Sparc20 work station using programs written in Matlab. Volumes of the viable and non-viable regions in each tumor were measured from the T_2-weighted images across the whole tumor. Since the tumor was grown in the thigh, no motion artifact was observed. Pixels that showed a higher signal intensity in the T_2-weighted images had a higher water content and, according to our previous experience, correlated with necrosis or edema, and classified as non-viable regions. Viable and non-viable regions were separated by threshold segmentation. Figure 1 shows an example of the segmentation analysis from one control tumor slice. In column 2 the non-viable region was outlined and superimposed on the T_2-weighted image. The Gd-DTPA-enhanced image is also shown in column 3. High signal intensity regions in the T_2-weighted images clearly correlate with low enhancement regions in the Gd-DTPA-enhanced images. The corresponding images from a similar location of this tumor in the week-1 and week-2 follow-up studies are also shown. Some regional resemblance seems to be maintained during tumor growth.

Viable, non-viable, and total volumes were calculated for each tumor by summing over the respective volumes measured from all images. The viable growth ratio was

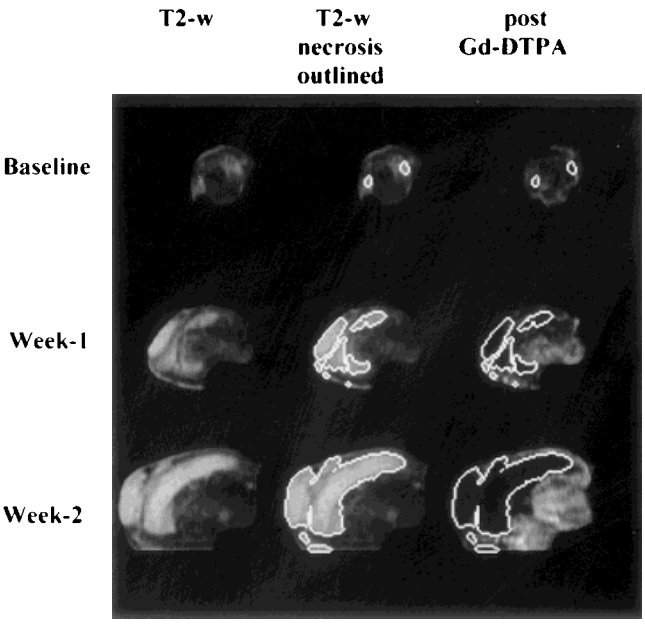

Figure 1. Images taken from a control tumor slice. Column one shows the T_2-weighted images, column two shows the outlined non-viable region defined as pixels with signal intensity higher than a threshold gray level, and column three shows the Gd-DTPA-enhanced images. High signal intensity regions in the T_2-weighted images (in column 2) are correlated with the low enhancement regions in the Gd-DTPA-enhanced images (in column 3). The second and third rows show the corresponding images from a similar location in this tumor at week-1 and week-2 follow-up studies. Some regional resemblance seems to be maintained while the tumor was growing larger.

defined as the viable tumor volume measured in the follow-up studies (week-1 and week-2) divided by its own baseline volume at baseline. Tumors with growth ratios measured at week 2 (10 days after treatment) that were comparable to the control tumors were classified as non-responders. Fifteen tumors were separated into three groups: controls, responders, and non-responders.

The following analyses of the contrast enhancement kinetics were based on the three groups. In each tumor, enhancement kinetics of the two agents were measured from every viable tumor pixel in the two slices selected for the dynamic study. The enhancement was calculated by subtracting the pre-contrast signal intensity from the post-contrast signal intensity. In the study of gadomer-17, the pre-contrast signal included the residual effect of Gd-DTPA, which was expected to remain at a stable level during the examination time of gadomer-17. By subtracting out the pre-contrast signal before the injection of gadomer-17, the residual effect of Gd-DTPA was accounted for. Non-viable regions in each slice, as determined from the corresponding T_2-weighted image, were excluded from the analysis.

Contrast enhancement kinetics in the liver of each animal were measured from a region of interest (ROI) placed in homogeneous liver parenchyma. The images acquired from liver did show some respiratory artifact (not severe). The major vessels causing the most artifact were excluded from the ROI. Enhancement kinetics from control and treated animals were averaged separately to calculate mean liver kinetics for each group. The signal enhancement decay rates in the liver (mono-exponential for gadomer-17, bi-exponential for Gd-DTPA) were used as the decay rates in the blood, which has been verified previously (6). After the decay rates for contrast agent in the blood concentrations were determined, a pharmacokinetic model was applied to analyze the enhancement kinetics to derive the parameters for vascular volume and permeability. The analysis was performed on a pixel-by-pixel basis. In addition, in each of the three groups the enhancement kinetics measured from all viable pixels were averaged to obtain mean tumor enhancement kinetics.

Pharmacokinetic Model

The details of the pharmacokinetic model employed have been described in a previous publication (12). Our model also reconciled with several major models, as described in a review paper by Tofts (14). Briefly, the model assumes two compartments in tissue, i.e., intravascular (blood) and extravascular (interstitial space). The transport of contrast agents between the two compartments is characterized by the fractional in-flux rate K_1 from the blood stream into the interstitial space and the fractional out-flux rate K_2 from the interstitial space back into the blood stream. The total concentration in a selected region of interest in tissue (eg, a pixel), C_T, contains contributions from the vascular and extravascular compartments. Mathematically, it can be expressed as $C_T = V_bC_b + V_eC_e$, where V_b is the blood volume, C_b is the concentration in blood, V_e is the distribution volume in the interstitial space, and C_e is the concentration in V_e. After the contrast agent was injected, its concentration in the vascular compartment was assumed to increase linearly from time 0 to a maximum value and then show subsequent decay. From one enhancement-time curve three independent parameters related to vascular volume (V_b), contrast agent accumulation rate in the interstitial space ($V_e K_1$), and the fractional out-flux rate from the interstitial space back to the bloodstream (K_2) can be computed using a non-linear least squares fitting algorithm. The enhancement in the liver is assumed to be proportional to its extracellular volume (assumed to be 24% [15]), which is used as a reference to convert the fitted vascular volume parameter to the fractional vascular volume V_b. In the analysis, the enhancement-time curve was fit directly to derive the model parameters. The implicit assumptions were that the enhancement was proportional to the concentration (problematic) and that the exchange between the vascular and extravascular compartments was slow (generally accepted; see the review paper by Donahue et al [16]). Technical issues related to the use of the signal enhancement curve have been discussed at length in a previous paper (6) and will not be repeated here.

Enhancement kinetics measured for each tumor were analyzed on a pixel-by-pixel basis. After the analyses were completed, the pixel population distribution curves of the parameters V_b and K_2 were computed, and based

on the curves measured in the baseline, longitudinal changes in week-1 and week-2 studies were assessed. Overall changes between control and treated groups were compared, as were the differences between responders and non-responders to determine whether the fitted parameters revealed a clear distinction between them and could thus serve as a predictor for therapeutic efficacy. The parameters measured by gadomer-17 and Gd-DTPA were also compared.

RESULTS

Viable Growth Ratio and Non-viable Volume Percentage

Chemotherapy caused severe systemic reactions in treated rats. In general, they were weaker (less active) and some died during the experimental period. All nine treated animals were alive at week 1, but only six rats in this group survived past week 2. The control rats, even though they bore large tumors, all survived to the end of the evaluation period.

Figure 2 shows the growth ratio of the viable tumor volume in the treated and control groups measured in the week-1 and week-2 studies. In the control group, the viable growth ratio was 2.9 ± 0.4 at week 1, and 6.6 ± 1.3 at week 2. One tumor in the treated group displayed a comparable growth rate as the control tumors did, and was therefore classified as a non-responder (NRS). The remainder of the treated tumors were defined as responders. Their viable growth ratio was 1.7 ± 0.1 at week 1, and 2.5 ± 0.6 at week 2. The viable growth ratios differed significantly between the control and responder groups. They were separated at week 2 by a threshold value of 4.0, with all controls above and all responders below that cut point.

Figure 3 shows the non-viable volume percentage (non-viable volume divided by the total volume) of tumors in the control, responder, and non-responder groups. Along with Fig. 2, these data show that the control tumors grew very rapidly, while the non-viable volume percentage slowly increased with time. The responders also grew, but at a slower rate and with a higher non-viable volume percentage.

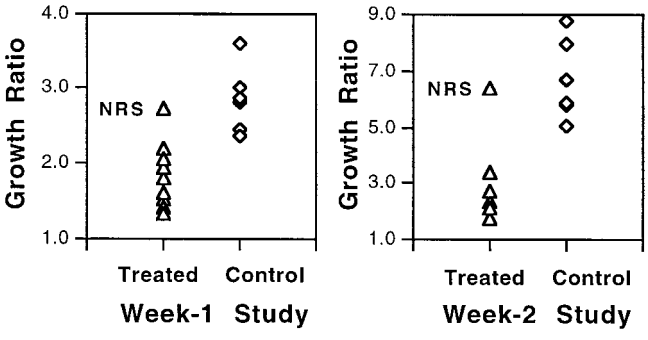

Figure 2. The growth ratio of the viable tumor volume in tumors in the treated and control groups measured at week 1 (left) and week 2 (right). One tumor in the treated group that displayed a growth rate comparable to that of the control tumors was classified as a non-responder (marked NRS). There were nine tumors in the treated group at week 1; only six rats had survived by week 2.

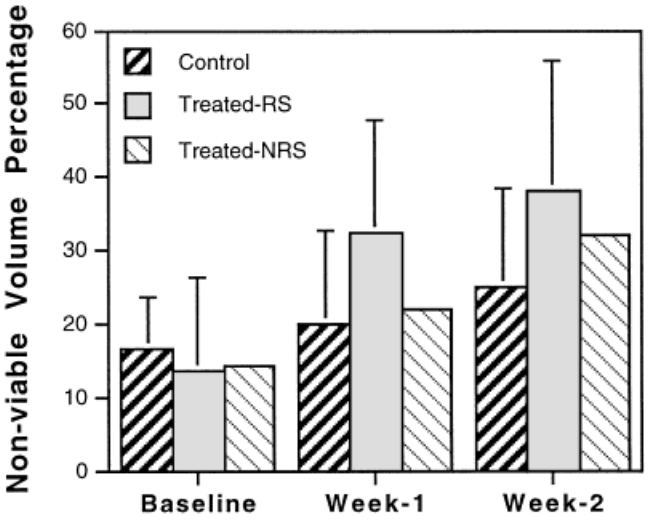

Figure 3. Percentage of non-viable volume in tumors in the control, responder, and non-responder groups measured in the baseline, week-1, and week-2 studies. Error bars represent the variations in each group. There was only one tumor in the non-responder group, thus no error bar. After the therapy the non-viable percentage increased more in the responders than in the controls.

Mean Enhancement Kinetics of Gadomer-17 and Gd-DTPA

In addition to structural changes, chemotherapy caused vascular changes. Figure 4 shows the mean enhancement kinetics measured by gadomer-17 from the three groups. The curve at each time point was obtained by averaging the kinetics of all viable pixels (400–3000 pixels in one tumor) from all tumors in that group. In the control group the kinetics measured at three time points exhibited similar magnitudes of enhancement. The only noticeable difference was that the decay rate at week 1 was more rapid. In the responder group, post-therapy enhancement at week 1 was lower compared with the baseline value. The enhancement decay rate at week 2 was substantially slower. Baseline kinetics in non-responders were much lower than in responders, and also the enhancement increased after therapy, two distinct features when compared with responders. Figure 5 shows the mean enhancement kinetics measured by Gd-DTPA in each group. Sequential contrast injection while the animal was fixed in the scanner made it possible to measure the kinetics of both agents from the same tumor regions in each group. In the responder group the difference of Gd-DTPA kinetics between the baseline and week-1 studies was much smaller than that measured by gadomer-17, but the difference became much larger by week 2. The baseline Gd-DTPA enhancement in the non-responder group was much lower than that in responders. The enhancement also increased at week 1 after treatment, but to a lesser degree compared with that measured by gadomer-17.

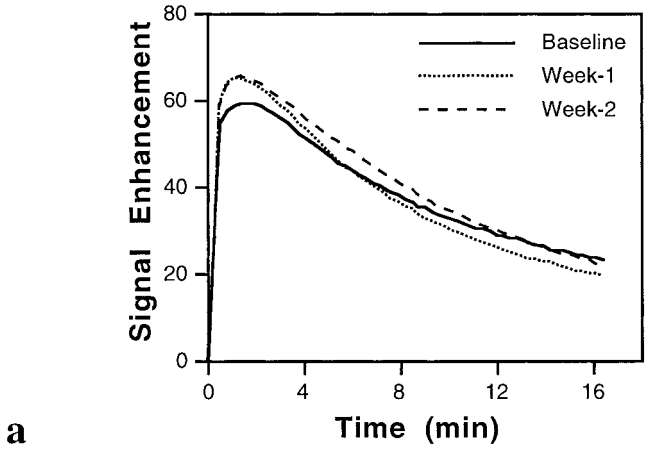

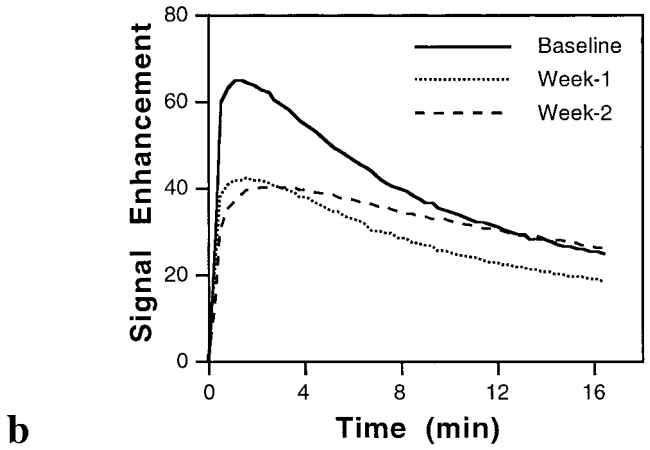

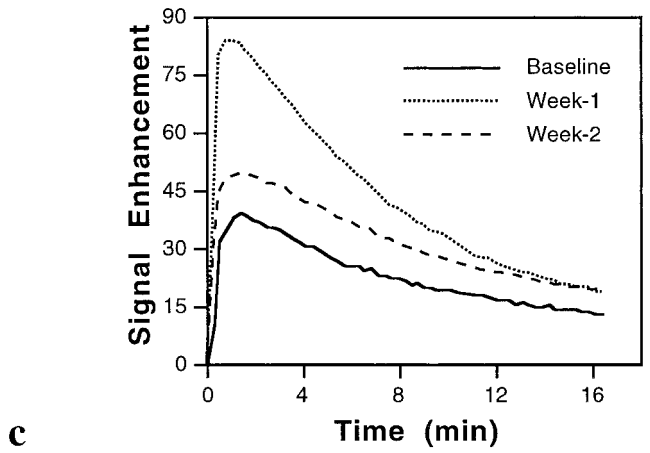

Figure 4. The mean enhancement kinetics measured by gadomer-17 from all viable tumor pixels in the control (**a**), responder (**b**), and non-responder (**c**) groups. In the control group, the kinetics measured at baseline, week 1, and week 2 were of similar magnitude, and the decay rate was faster at week 1. In the responder group, enhancement measured by gadomer-17 decreased after therapy. In the non-responder group, baseline enhancement was much lower than that in the controls or responders, and the enhancement became even greater after therapy.

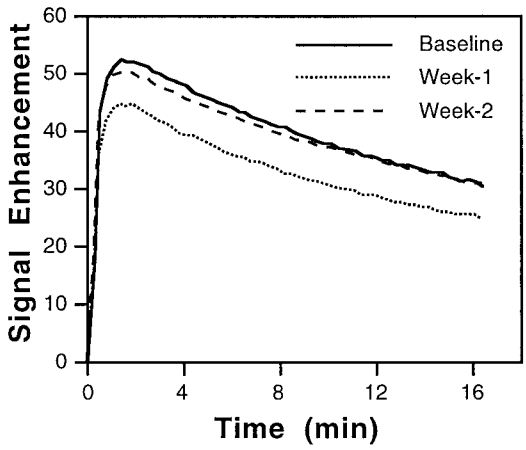

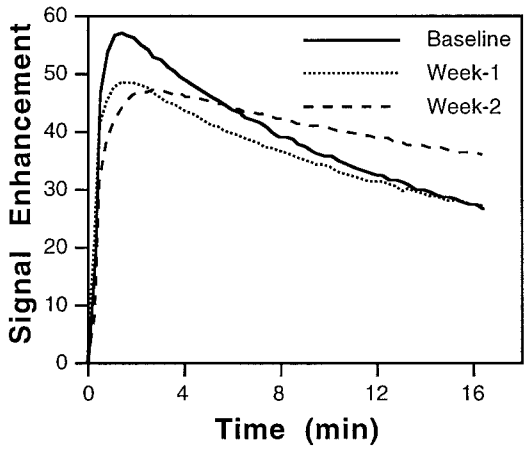

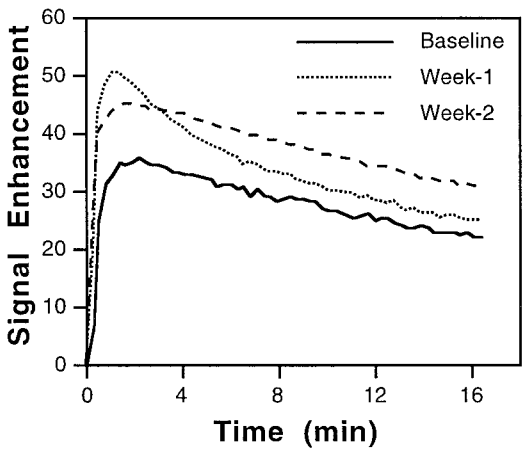

Figure 5. Mean enhancement kinetics measured by Gd-DTPA from all viable tumor pixels in the control (**a**), responder (**b**), and non-responder (**c**) groups. The pixels were the same as those in Fig. 4 as measured by gadomer-17. The changes between baseline and week-1 studies were similar in the control and responder groups and thus could not be used to differentiate these two groups. In the non-responder, baseline enhancement was much lower than that in the controls or responders, and enhancement also became greater after the therapy, similar to the results measured by gadomer-17.

Decay Rates in Liver Kinetics

Decay rates in blood concentrations were determined from the decay rates in enhancement kinetics measured from the liver. The kinetics were similar to what we previously found for Gd-DTPA-24-cascade-polymer and Gd-DTPA (6). The decay kinetics for gadomer-17 were assumed to be mono-exponential, while Gd-DTPA kinetics were bi-exponential. The exponential decay rates in the control and treated groups at the three experimental time points are listed in Table 1. Based on the single decay rate of gadomer-17, in the control groups the decay rates were similar at baseline and week 1, but became slower at week 2. In the treated group, decay rates were slower at week 1, and even slower at week 2. Decay rates of Gd-DTPA basically followed a similar trend.

Vascular Volume V_b Derived From Gadomer-17 Kinetics

After the decay rates in blood concentrations were determined, pharmacokinetic analysis was performed to derive the three parameters in each pixel, and the pixel population distribution curves of V_b and K_2 were calculated for each tumor. The results for another parameter, V_eK_1, were also obtained. However, the data did not show any significant change at the three time points. Also, since they involved two parameters (V_e and K_1), the data were more difficult to interpret. Therefore, the results are not presented.

For V_b and K_2, the group population distribution curves were calculated by pooling together all tumors in each of the control, responder, and non-responder groups. Figure 6 shows the pixel population distribution curve of the fractional vascular volume (V_b) in the control and responder groups calculated from the kinetics of gadomer-17. In the control group (Fig. 6a), median fractional vascular volume was 8.8% at baseline, dropping slightly to 7.8% at week 1, and remaining at 7.8% by week 2. These changes were not significant. The median fractional vascular volume of the responder group was 10% at baseline, dropping to 5.4% at week 1 ($P < 0.005$), and to 3.7% at week 2 ($P < 0.0005$). Vascular volume in non-responders increased after treatment. The median fractional vascular volume was 4.6% at baseline, increasing to 8.5% at week 1, and then dropping to 4.4% by week 2. However, since there was only one non-responding tumor, statistical analysis could not be performed. These results indicate that the evolution of the vascular volume distribution in responders and non-responders could be differentiated from that of the controls.

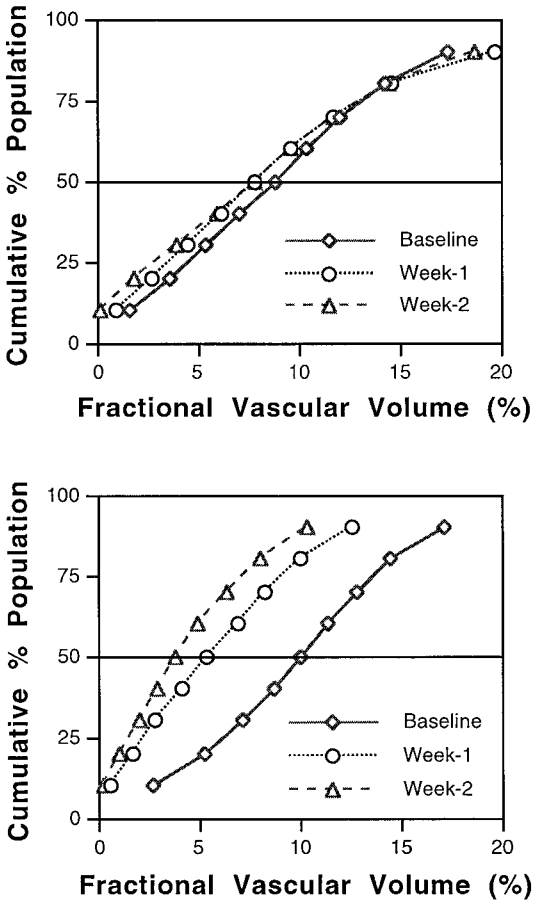

Figure 6. Pixel population distribution curve of the fractional vascular volume(V_b) in the control (**a**) and responder (**b**) groups, as calculated from the kinetics of gadomer-17. The horizontal axis is the fractional vascular volume in each pixel, and the vertical axis is the cumulative percent of pixels. The median line (50% population) is also marked. In the control group the median fractional vascular volume changed from 8.8% in the baseline to 7.8% at week 1 and week 2 (non-significant). In the responder group the median fractional vascular volume changed from 10% in the baseline to 5.4% at week-1 ($P < 0.005$) and to 3.7% at week 2 ($P < 0.0005$).

Fractional Out-flux Rate K_2 Derived From Gadomer-17 Kinetics

Figure 7 shows the pixel population distribution curve of the fractional out-flux rate K_2 derived from ga-

Table 1
Exponential Decay Rates in the Mean Liver Enhancement Kinetics Measured by Gadomer-17 (Mono-exponential) and Gd-DTPA (Bi-exponential) in the Control and Treated Groups*

	Gadomer-17			Gd-DTPA		
	Baseline	Week 1	Week 2	Baseline	Week 1	Week 2
Control	0.196	0.188	0.140	60% 1.472 40% 0.09	57% 1.362 43% 0.091	52% 1.128 48% 0.052
Treated	0.204	0.144	0.115	58% 1.356 42% 0.093	51% 1.132 49% 0.073	51% 1.13 49% 0.07

*The bi-exponential decay function was defined as $f_1 \exp(-\alpha_1 t) + f_2 \exp(-\alpha_2 t)$, where f_1 and f_2 are the relative weighting factors, given as the percentage in the table. The exponential decay rate unit is 1/min. The variation in each study group is 8% to 10%.

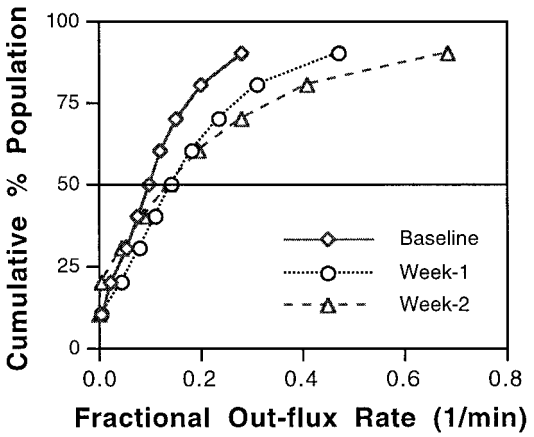

a

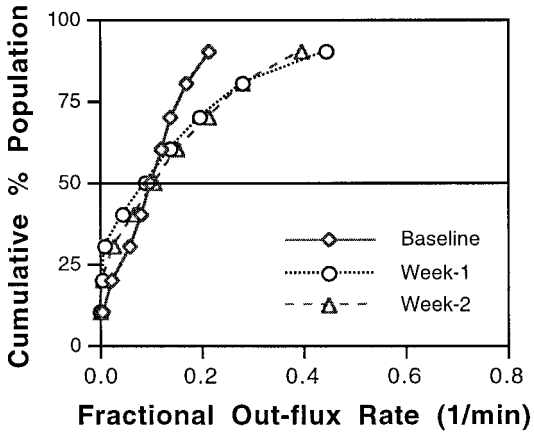

b

Figure 7. Pixel population distribution curve of the fractional out-flux rate (K_2) in the control (**a**) and responder (**b**) groups, derived from gadomer-17 kinetics. In the control group one notes that the population distribution curve above the median line at week 1 was shifted to higher values compared with that in the baseline, and at week 2 a further shift was noted. Above the median line the changes were significant. In the responder group, above the 60% population line one can note a shift toward higher values in the follow-up studies compared with the baseline, but there is no difference between week-1 and week-2 studies.

domer-17 kinetics. Control tumors grew very rapidly, and Fig. 7a demonstrates that the population distribution above the median at week 1 was shifted to higher values compared with baseline, and a further shift was noted at week 2. Statistical analysis revealed that the median K_2 value did not show significant longitudinal changes, but for pixels above the median line the changes were significant. In the responder group (shown in Fig. 7b), a shift toward higher values was noted above the 60% population line in the follow-up studies compared with the baseline, but no difference was seen between week-1 and week-2 studies.

Comparison Between the Two Contrast Agents

Enhancement kinetics measured by Gd-DTPA were analyzed in a similar fashion. Pixel population distribution curves of fractional vascular volume(V_b) and fractional out-flux rate (K_2) were obtained, and longitudinal changes were analyzed within each group. In the gadomer-17 study, results for vascular volumes (Fig. 6) demonstrated that the changes in the top half (above median line) and bottom half (below median line) of the population were similar, but results for the fractional out-flux rate (Fig. 7) showed that major changes were taking place in the top half of the population. Therefore, in the following analysis for V_b we focus on the whole pixel population, whereas for K_2 we only focus on the top half-pixel population. Longitudinal changes measured at week 1 and week 2 were compared with baseline values. Table 2 summarizes the percent change of the mean V_b value in the whole population and the mean K_2 in the top half of the population measured by using both contrast agents. The degree of statistical significance assessed by using paired t-test was also determined.

The mean vascular volume in the control group was not significantly changed at week 1 or week 2, as measured by both contrast agents. However, in the responder group, vascular volume measured by gadomer-17 revealed a 42% decrease, while that measured by Gd-DTPA did not show a significant change at this time point. By week 2, vascular volume measured by gadomer-17 showed a further decrease (56%), and that measured by Gd-DTPA also revealed a significant (47%) decrease. Therefore, the results indicated that by week 2, i.e., 10 days after therapy, both gadomer-17 and Gd-DTPA could detect the vascular changes, but at an earlier time (week 1, 4 days after therapy) only gadomer-17 could reveal the change.

Analysis of the fractional out-flux rate K_2 measured by gadomer-17 revealed significant increases in both control and responder groups, which were not detected by Gd-DTPA. The mean K_2 value in the top half population of the control group showed a 58% increase at week 1, with a further increase to 105% at week 2. The fractional out-flux rate K_2 is a parameter of vascular permeability, when perfusion is sufficiently high (see more detailed discussion later). Therefore, the results indicate that vascular permeability increased in the control tumors, greater at week 2 compared with week 1. In the responder group, there was also a significant increase in vascular permeability after therapy, with a similar increase at week 1 and week 2 (about 60% increase). This may also be interpreted as increased

Table 2
Percentage Changes of the Mean Fractional Vascular Volume (V_b) in the Whole Population and the Mean Fractional Out-flux Rate (K_2) in the Top Half Pixel Population in the Week-1 (W1) and Week-2 (W2) Studies Compared With Baseline (B/L)

	Vascular volume (V_b)		Out-flux rate (K_2)	
	Gadomer-17	Gd-DTPA	Gadomer-17	Gd-DTPA
Control				
W1 vs. B/L	−3	−20	+58**	+10
W2 vs. B/L	−8	−7	+105*	+24
Responder				
W1 vs. B/L	−42**	−7	+60*	−5
W2 vs. B/L	−56**	−42**	+59*	−13

*$P < 0.05$.
**$P < 0.005$.

vascular permeability in certain regions of the tumor after chemotherapy.

DISCUSSION

Assessment of Therapy Efficacy and Hemodynamic Changes in the Host Animal

The chemotherapy regimen (mitomycin-C with FAA) used in this study worked well in the R3230 AC tumor model. In the analysis, responders and non-responders were defined by comparing their growth rates with that of control tumors. Although tumor regression did not occur, most of the treated tumors (eight of nine) did show a slower growth rate than controls. The high mortality rate by week 2 (three of nine) indicates that the regimen was toxic. However, our purpose was not to test the efficacy of the regimen itself, but to create a successful treatment model to explore the vascular changes taking place in the responders and non-responders versus the controls.

The host animal showed some longitudinal changes in its clearance efficiency of the contrast agents. The hemodynamic changes in the host animal were measured from the liver kinetics. The rising phase in the liver kinetics were similar at the three time points; the decay rates showed substantial changes, and they were used in the pharmacokinetic analysis at different experimental time points to account for the changes in the host. In the treated group the change taking place after therapy (week 1) was presumably due to the effect of the drugs, and the change in the control groups at week 2 was probably due to the large tumor burden. The slower decay curves in tumor kinetics at week 2 shown in Figs. 4 and 5 were influenced by the slower clearance of the contrast agents in the blood. By incorporating these hemodynamic changes into the analysis, the changes due to the weakened state of the host animals could be accounted for.

Pharmacokinetic Model and Interpretation of the Derived Parameters

Enhancement kinetics were analyzed by a pharmacokinetic model to derive characteristic parameters related to vascular volume and permeability. In a review by Tofts (14), the three major pharmacokinetic models developed by Tofts and Kermode (17), Larsson et al (18), and Brix et al (19) were reconciled. The parameters used in our model were comparable to theirs. For example, our parameter K_2 is the same as the parameter k_{ep} (= $k_{out}^{PS_P}/V_e$) in Toft and Kermode's review, which is also the parameter EF/v in the model of Larsson et al (18) and the parameter k_{21} in the model of Brix et al (19); also our K_2 is analogous to the fractional leak rate from the interstitial water to plasma, FLR_{out} in the model of Shame et al (20). Therefore the parameters and notations used in the present work can be easily compared with those reported by other groups.

Although kinetic parameters are reconcilable among the major models, fundamental problems with the pharmacokinetic modeling analysis have not been resolved. Three major factors determine the kinetics of contrast agents in a tissue: blood perfusion, transport of agents across the vessel wall (via diffusion or convection), and diffusion of agents in the interstitium. If the agents delivered by blood are not sufficient, it will be the dominant factor determining the agent kinetics in the tissue. As we have previously demonstrated, the kinetics measured in necrotic or semi-necrotic regions are mainly dependent on perfusion (12). If perfusion is sufficient, transport across the vessel wall is the second factor to determine the agent kinetics. For the two agents used in this study, diffusion is the major mechanism for transendothelial transport, which is described by permeability-surface area product (PS) (21). The third factor is the interstitial diffusion of agents away from the vascular space (22). Although these three physiological parameters cannot be clearly separated in the measured pharmacokinetics, they have to be considered when trying to interpret the derived pharmacokinetic parameters.

Interpretation of the Derived Parameter V_b as the Vascular Volume

The initial rise phase in the measured enhancement after contrast agent injection is attributed to vascular distribution. However, our previous experience in analyzing the kinetics of Gd-DTPA and other macromolecular contrast agents, including Gd-DTPA-24-cascade-polymer (30 kD), polylysine-Gd-DTPA (50 kD), and albumin-Gd-DTPA (13,23), has demonstrated a basic problem with the measurement of vascular volume, that is, it actually contained an apparent vascular volume, which included the true vascular volume, and the fast leakage volume into the interstitial space. The problem is more severe when using a smaller agent than a macromolecular agent.

V_b in Responders/Non-responders Compared With Controls

Based on the tumors' growth rates in the week-2 study (i.e., 10 days after the therapy), the responders could be separated from the controls and the single non-responder. Although we used the results of tumor growth at week 2 to separate the responders from non-responders, we focused our attention on the differential changes taking place between the baseline and week-1 studies to assess the tumor response at an earlier time. If the outcome can be predicted soon after the administration of therapy, it may allow for early intervention in case of treatment failure. One significant difference between the responders and the non-responder was the vascular volume at baseline, as demonstrated in Figs. 4 and 5. The non-responder had a much lower baseline vascular volume than that of the responders. The median vascular volume as determined from the kinetics of gadomer-17 was 4.6% in the non-responder and 10% in the responders. Vascular volume is a critical determinant for the delivery of therapeutic drugs into the tumor (24). The non-responder had a much lower vascular volume, which may have limited drug delivery and resulted in treatment failure. The next distinctive difference between the two groups was the change in vascu-

lar volume at 4 days after therapy compared with their baseline values. The median vascular volume derived from the kinetics of gadomer-17 showed a 46% (from 10% to 5.4%) decrease in responders, while it increased in the non-responder. Therefore, low vascular volume before treatment and increased vascular volume after the treatment seemed to predict treatment failure. However, since only one non-responder was found in this study, this needs to be verified with additional studies. In support of our results, Reddick et al (25) have reported a similar finding in patients with osteosarcoma as measured with dynamic contrast-enhanced MRI longitudinally during the course of therapy. Tumors with a steeper enhancement slope and/or maximum enhancement at presentation had greater decreases in that parameter over the course of chemotherapy. The greater change was correlated with increased tumor necrosis.

The changes of vascular volume as measured by gadomer-17 also showed a clear distinction between responders and controls, with a 46% decrease vs. a non-significant change in the median vascular volume (or, a 42% decrease vs. a non-significant change in the mean vascular volume). Thus, vascular volume seemed to be a good predictor of tumor growth rates after 1 week at week 2. Decreased vascular volumes in the responder group were correlated with the decrease in their volumetric growth (with a viable growth ratio of 2.5 ± 0.6) compared with the controls (6.6 ± 1.3). In contrast, the vascular volume derived from the kinetics of Gd-DTPA measured at week 1 did not reveal any significant change in either group and failed to predict the difference in tumor growth between these two groups. As mentioned previously, the vascular volume actually contained a true vascular volume and a fast leakage volume in the interstitial space, and the problem was more severe with smaller agents, which may be the reason that Gd-DTPA is not able to detect the decrease of vascular volume after therapy. However, at week 2 Gd-DTPA did show a significant decrease in the responders compared with the controls. The results suggest that, compared with macromolecular agents, Gd-DTPA could detect the changes of vascular volume later in terms of time and with less sensitivity.

Interpretation of K_2 as Vascular Permeability

The other parameter analyzed in the model is the fractional out-flux rate K_2, which is a measure of how fast the agent diffuses from the interstitial space back to the blood stream. This parameter is dependent on the vascular permeability and diffusion of the agent in the interstitial space back to the vascular space. Therefore interpretation of K_2 as vascular permeability must be taken cautiously. As discussed earlier, when perfusion is sufficient, the K_2 rate is dependent on the vascular PS. If not, the situation becomes complicated. We have previously shown that when the kinetics measured from necrotic regions were analyzed with the pharmacokinetic model, we obtained a result of $V_b = 0$ and $K_2 = 0$ (12). The permeability in necrotic regions might be high, but sufficient levels of contrast agents could not be delivered into this region to detect it, resulting in a low K_2 value. If this factor was not taken into account, the low K_2 would be misinterpreted as low permeability. Therefore, in the analysis we focused on the top half population with relatively high K_2, excluding the bottom half population to minimize the problem.

K_2 in Controls and Responders

Control tumors presented a relatively fast growth rate with a mean viable volumetric growth ratio of 2.9 ± 0.4 at week 1, and 6.6 ± 1.3 at week 2. Thus, they were an excellent model for investigation of parameters sensitive to aggressive growth. The fractional out-flux rate K_2 as determined from the kinetics of gadomer-17 seemed to correlate well with the growth rates over time. The mean K_2 value in the top half of the population showed a 58% ($P < 0.005$) increase at week 1 and a 105% ($P < 0.05$) increase by week 2, indicating that increased out-flux transport rate K_2 is associated with rapid tumor growth. In recent years much evidence has been published to support the notion that vascular permeability is related to angiogenesis, an essential process for the growth of tumors, and that information on permeability can be measured with dynamic contrast-enhanced MRI by using macromolecular contrast agents (5,26). The connection between angiogenesis and vascular permeability is believed to be mediated by the presence of VPF or VEGF (7,8).

In the responder group, the mean K_2 in the top half population also increased significantly. The results could be related to the known effects of the therapeutic drug FAA (27). Vascular permeability might increase due to initial drug intervention; later the vessels collapsed and resulted in a decreased vascular volume. Therefore, we could state with confidence that the vascular permeability increased in certain regions of the treated tumors. The attempt to relate the K_2 rates derived from the kinetics of Gd-DTPA to the vascular permeability was even more problematic (6). The percent change in either the control or the responder groups was much smaller than those measured by gadomer-17 and not statistically significant. Therefore, Gd-DTPA could not be used to detect the vascular permeability changes.

Measurements of Vascular Permeability With Different Sized Agents

The above analyses and discussion were based on selective measurements from the viable regions of the tumor. If the non-viable regions were not excluded in the analysis, the results would be heavily biased by their poor vascular structure, and consequently the information on vascular permeability would become even more difficult to obtain. The assessment of the vascular permeability in a system with highly permeable vessels based on the use of small contrast agents is a very difficult task and often not reliable. Therefore, a larger macromolecular agent, such as albumin-Gd-DTPA, is probably the best choice in this situation. As has been demonstrated in the literature, dynamic contrast-enhanced MRI with albumin-Gd-DTPA could reveal permeability changes in tumors treated with tumor necrosis factor alpha (28) and radiation therapy (9,10). It could also differentiate the degrees of vascular permeability in various disease models (29), as well as tumor

grades in a mammary tumor model (30). However, the low binding efficiency (thus excess albumin has to be used) and the long retention of this agent in the body currently disqualify it for human use. Therefore, the vascular permeability measured by an intermediate size agent (such as the dendrimer-based compound gadomer-17 used in this study) might have a valuable clinical application in the future.

CONCLUSIONS

In this study we investigated the longitudinal structural and vascular changes in control and chemotherapy-treated tumors. We found out that vascular volume derived from the kinetics of the intermediate size agent gadomer-17 could serve as an early predictor for treatment efficacy. Responders, defined by their slower growth rates compared with controls, showed significantly decreased vascular volumes at 4 days after the therapy. The only non-responder in this study showed an increased vascular volume after therapy. Gadomer-17-based dynamic MRI detected the changes earlier and with a greater sensitivity than Gd-DTPA-based imaging. In the control tumors, changes in the fractional out-flux rate K_2 of gadomer-17 correlated with tumor growth rate and could potentially serve as an indicator for the aggressiveness of tumor growth.

ACKNOWLEDGMENTS

The authors thank Schering AG and Dr. H.-J. Weinmann for providing the macromolecular contrast agent gadomer-17 and for useful discussions. We thank Dr. R. Weissleder from the Massachusetts General Hospital for providing us with the R3230 AC tumor line. We also thank Dr. Xiaoyan Lao for her skillful technical assistance in the animal studies and Dr. John Fruehauf for reviewing the manuscript.

REFERENCES

1. Fletcher BD, Hanna SL, Fairclough DL, Gronemeyer SA. Pediatric musculoskeletal tumors: use of dynamic, contrast-enhanced MR imaging to monitor responses to chemotherapy. Radiology 1992;184: 243–248.
2. Bonnerot V, Charpentier A, Frouin F, Kalifa C, Vanel D, Di Paola R. Factor analysis of dynamic magnetic resonance imaging in predicting the response of osteosarcoma to chemotherapy. Invest Radiol 1992;27:847–855.
3. Evelhoch J, Cunnings A, Lucas D, et al Early detection of therapeutic response by dynamic contrast-enhanced MRI. In: Proceedings of an ISMRM Workshop: MR of Cancer: Physiology and Metabolism, Baltimore, MD, 1996. p 61.
4. Heywang-Koebrunner SH, Viehweg P. Sensitivity of contrast-enhanced MR imaging of the breast. Magn Reson Imaging Clin North Am 1994;2:527–38.
5. van Dijke CF, Brasch RC, Roberts TP, et al Mammary carcinoma model: correlation of macromolecular contrast-enhanced MR imaging characterizations of tumor microvasculature and histological capillary density. Radiology 1996;198:813–818.
6. Su MY, Mühler A, Lao X, Nalcioglu O. Tumor characterization with dynamic contrast enhanced MRI using MR contrast agents of various molecular weights, Magn Reson Med 1998;39:259–269.
7. Dvorak HF, Brown LF, Detmar M, Dvorak AM. Vascular permeability factor/vascular endothelial growth factor, microvascular hyperpermeability, and angiogenesis. Am J Pathol 1995;146:1029–1039.
8. Claffey KP, Robinson GS. Regulation of VEGF/VPF expression in tumor cells: consequences for tumor growth and metastasis. Cancer Metast Rev 1996;15:165–176.
9. Cohen FM, Kuwatsuru R, Shames DM, et al Contrast-enhanced magnetic resonance imaging estimation of altered capillary permeability in experimental mammary carcinomas after X-irradiation. Invest Radiol 1994;29:970–977.
10. Schwickert HC, Stiskal M, Roberts TP, et al Contrast-enhanced MR imaging assessment of tumor capillary permeability: effect of irradiation on delivery of chemotherapy. Radiology 1996;198:893–898.
11. Knopp MV, Brix G, Junkermann HJ, Sinn HP. MR mammography with pharmacokinetic mapping for monitoring of breast cancer treatment during neoadjuvant therapy. Magn Reson Imaging Clin North Am 1994;2:633–658.
12. Su MY, Jao JC, Nalcioglu O. Measurements of vascular volume fraction and blood-tissue permeability constants with pharmacokinetic model: studies in rat muscle tumor. Magn Reson Med 1994;32: 714–724.
13. Su MY, Najafi AA, Nalcioglu O. Regional comparison of tumor vascularity and permeability parameters measured by albumin-Gd-DTPA and Gd-DTPA. Magn Reson Med 1995;34:402–411.
14. Tofts PS. Modeling tracer kinetics in dynamic Gd-DTPA MR imaging. J Magn Reson Imaging 1997;7:91–101.
15. Donahue KM, Weisskoff RM, Parmelee DJ, et al Dynamic Gd-DTPA enhanced MRI measurement of tissue cell volume fraction. Magn Reson Med 1995;34:423–432.
16. Donahue KM, Weisskoff RM, Burstein D. Water diffusion and exchange as they influence contrast enhancement, J Magn Reson Imaging 1997;7:102–110.
17. Tofts P, Kermode A. Measurement of the blood-brain barrier permeability and leakage space using dynamic MR imaging. 1. Fundamental concepts. Magn Reson Med 1991;17:357–367.
18. Larsson H, Stubgaard M, Frederiksen J, Jensen M, Henriksen O, Paulson O. Quantitation of blood-brain barrier defect by magnetic resonance imaging and gadolinium-DTPA in patients with multiple sclerosis and brain tumors. Magn Reson Med 1990;16:117–131.
19. Brix G, Semmler W, Port R, Schad L, Layer G, Lorenz W. Pharmacokinetic parameters in CNS Gd-DTPA enhanced MR imaging. J Comput Assist Tomogr 1991;15:621–628.
20. Shames D, Kuwatsuru R, Vexler V, Muhler A, Brasch RC. Measurement of capillary permeability to macromolecules by dynamic magnetic resonance imaging: a quantitative noninvasive technique. Magn Reson Med 1993;29:616–622.
21. Jain RK. Transport of molecules across tumor vasculature. Cancer Metast Rev 1987;6:559–593.
22. Baxter LT, Jain RK. Transport of molecules in the tumor interstitium: a review. Cancer Res 1987;47:3039–3051.
23. Su MY, Lao X, Nalcioglu O. Quantitative comparison of pharmacokinetics of polylysine-Gd-DTPA, Gd-DTPA-24-cascade-polymer, and Gd-DTPA in blood, liver, and tumor of rats. In: Proceedings of the 4th SMR Annual Meeting, New York, 1996. p 1697.
24. Jain RK. Physiological resistance to the treatment of solid tumors. In: Teicher BA, editor. Drug resistance in oncology. New York: Marcel Dekker; 1993. p 87.
25. Reddick WE, Bhargava R, Taylor JS, Meyer WH, Fletcher BD. Dynamic contrast-enhanced MR imaging evaluation of osteosarcoma response to neoadjuvant chemotherapy. J Magn Reson Imaging 1995;5:689–694.
26. Brasch RC, Pham C, Shames D, et al Assessing tumor angiogenesis using macromolecular MR imaging contrast media. J Magn Reson Imaging 1997;7:68–74.
27. Peters CE, Trotter MJ, Chaplin DJ. Early spatial and temporal changes in tumour perfusion after administration of flavone acetic acid. Int J Radiat Biol 1991;60:41–48.
28. Aicher KP, Dupon JW, White DL, et al Contrast-enhanced magnetic resonance imaging of tumor-bearing mice treated with human recombinant tumor necrosis factor alpha. Cancer Res 1990;50: 7376–7381.
29. Demsar F, Roberts TP, Schwickert HC, et al A MRI spatial mapping technique for microvascular permeability and tissue blood volume based on macromolecular contrast agent distribution. Magn Reson Med 1997;37:236–242.
30. Daldrup HE, Brasch RC, Muehler A, et al MRI quantification of tumor microvascular permeability using macromolecular contrast media: comparison between Gd24-cascade-polymer and albumin-Gd-DTPA. In: Proceedings of the 5th ISMRM Annual Meeting, Vancouver, B C, Canada, 1997. p 1592.